# The -stable region analysis in dynamic downlink cellular networks

Qiong Liu, Jean-Yves Baudais, Philippe Mary

# The $\epsilon$-stable region analysis in dynamic downlink cellular networks

Qiong Liu, Jean-Yves Baudais, Philippe Mary
Univ Rennes, INSA Rennes, CNRS, IETR-UMR 6164, F-35000 Rennes, France
Email: qiong.liu@insa-rennes.fr

***Abstract*—In this work, we give a complete characterization of the $\epsilon$-stable region in dynamic downlink random cellular networks. The $\epsilon$-stable region is the set of arrival rates such that the proportion of unstable queues in the network is not larger than $\epsilon$. We derive upper and lower bounds as well as an approximation of the critical arrival rate, which delimits the $\epsilon$-stable region. The developed model is based on stochastic geometry and queuing theory to handle the interaction between the transmit success probability and the queuing state evolution. Extensive numerical simulations are provided to confirm the tightness of the approximation.**

***Index Terms*—Stochastic geometry, queuing theory, $\epsilon$-stable region, Gil-Pelaez Theorem.**

## I. Introduction

Stochastic geometry provides a mathematical framework to analyze the performance of large scale wireless networks by capturing the spatial randomness intrinsic to the wireless systems including fading, shadowing, and power control [1], [2]. In the last decade, stochastic geometry has been combined with various complex network models taking into account frequency reuse, multiple antennas, multiple-tiers, or load-aware protocols, to cite a few [2]–[5].

However, most of the literature relies on the assumption that the transmitters are backlogged, i.e., the transmitters always have packets to transmit in their buffer. This full load assumption leads to pessimistic estimates of the system performance. Since the real systems are subject to temporal traffic variations and the signal sources generate packets according to some stochastic process, the load-awareness is essential for real-world performance assessment [3]. However, the interaction between buffers, or queues, at each transmitter makes the problem mathematically rather involved, because the state of each queue depends on the state of all others queues. The analysis remains however challenging due to the complex interactions: the amount of active BS at a time, which depends on the arrival rate, determines the level of interference in the network. This interference level determines the successful transmission rate of each BS that governs each buffer state, that, at the end, impacts the amount of active BS. These interactions make the queues closely dependent on each other.

A first attempt combining stochastic geometry and queueing theory has been granted in [3], where the coverage probability considering load has been investigated. In the case where each transmitter provides a buffer for queueing, the primal consideration is about queueing stability. For a point-to-point system with random arrival and departure processes at the BS, the queue stability requires that the service rate be larger than the arrival rate [6]. However, traffic conditions are more complicated in a large-scale network with multiple queues since the service rate depends on the state of all transmitters in the network. To address this issue, recent attempts have been made in [7]–[10]. The stability of uplink random access networks have been studied in [7]. However, a single cell network has been considered in this work thereby ignoring the inter-cell interference. A traffic-aware spatio-temporal model for uplink cellular networks has been developed in [8] to study the scalability and stability tradeoff, i.e., its ability to support a large number of devices while the queue sizes are not diverging. In [9], the network stable region in a downlink cellular network has been investigated. The main drawback of these results is that they only consider the average performance based on the first statistical moment of useful metrics, i.e., the coverage probability. These metrics provide limited amount of information. For example, given a packet arrival rate of $0.4$, and a coverage probability of $0.5$, i.e., the probability that the signal to interference plus noise ratio (SINR) of the typical user exceeds a given threshold $\theta$ is 0.5, the network is said to be stable since the coverage probability is larger than the arrival rate. However, half of the users could have a coverage probability of $0.8$ and another half of $0.2$, then only the user with the coverage probability of $0.8$ are stable, i.e., half of the users. The other extreme case is that all users have a coverage probability of $0.5$, which indicates that all the users are stable. Clearly, both situations lead to the same average coverage probability among users, but they correspond to a quite different users experience.

To overcome this drawback, a more refined metric known as $\epsilon$-stable region has been proposed in [10]. Unlike the stability region, that is based on the first moment measure, $\epsilon$-stable region relies on the moment generating function of the signal to interference plus noise ratio (SINR). The characterization of the $\epsilon$-stable region relies on the meta distribution [11]. This concept allows to answer the question "What is the set of arrival rates such that the proportion of unstable queues in the network is below $\epsilon$ at a required SINR?". It is worth noting the similarity between this definition and the $\epsilon$-capacity one: the latter gives the maximum achievable rate at which the probability being in outage is lower than $\epsilon$. A single letter characterization of the $\epsilon$-stable region is, however, far from

This work has been funded by a China Scholarship Council (CSC) grant.

being trivial because of the interactions between the queues. To overcome this problem, upper and lower bounds have been proposed to analyze the $\epsilon$-stable region, and to avoid the effect of queue interaction [10]. However, the bounds are not very tight especially under some network configurations.

The main contributions of this paper can be summarized as follow. First, we provide the closed-form expression of the upper and lower bounds of $\epsilon$-stable region in the case of random link distances, contrary to [10] where the communication distance is fixed. Moreover, unlike our previous work in [9] where only stable region was considered, in this paper we focus on the $\epsilon$-stable region to characterize the probability that a queue in the network be unstable is below $\epsilon$. Second, we propose an alternative definition of the $\epsilon$-stable region and derive accordingly a tight approximation of the critical arrival rate that was unavailable in literature. In particular, a discrete time Markov chain (DTMC) is used to handle the interaction between the transmit success probability and the queue state evolution to obtain the tight approximation of the critical arrival rate, contrary to the bounds provided in literature where the interaction between queues is not considered. Our result reveals that the proposed approximation is tighter than the bounds.

Throughout the paper, $\mathbb{P}(\cdot)$ denotes the probability under the underlying distribution, $\mathbb{E}_X(\cdot)$ denotes the expectation over the random variable $X$, $\mathrm{Im}\{\cdot\}$ represents the imaginary part of a complex number. The indicator function is denoted as $\mathbb{1}(A)$, which takes values 1 when the proposition $A$ is true and 0 otherwise. The Euclidean norm is denoted as $\|\cdot\|$.

## II. System model

### A. Network topology

A single-tier downlink cellular network is considered whose base stations (BSs) lie in $\mathbb{R}^2$ following an independent and homogeneous Poisson point process (HPPP) $\Phi$, with intensity $\lambda$. User equipment (UE) density is high enough such that every BS has at least one UE associated with it. Besides, each UE is associated to the closest BS. A single UE is randomly chosen as the typical UE, and we further assume that it is located at the origin for the ease of analyses. Moreover, all BSs are assumed to transmit in the same band, i.e., using a full frequency reuse approach. A block-fading propagation model is considered, where the channels between any pair of transceivers are assumed independent and identically distributed (i.i.d.) and quasi-static, i.e., the channel is constant during one transmission slot, and varies independently from slot to slot.

The arrival and departure traffic per BS are discrete stochastic processes. The time is slotted in very short equal intervals in which only one packet arrives or leaves from the BS queues in the network. This model is widely used in literature [8], [12], [13]. The packet arrival process at each transmitter is assumed to be a Bernoulli process with a rate $\xi \in [0, 1]$ expressed in packet per slot and per BS. Without loss of generality, we assume the packet size is fixed and it requires exactly one time slot to be transmitted. Each BS maintains an independent queue of infinite size to store the generated packets.

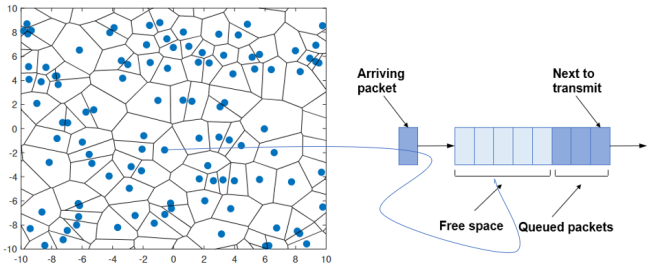


Figure 1. Realization of an HPPP with evolution of the queue in each transmitter.

Contrarily to the arrival process, the departure process cannot be fixed *a priori*. It is characterized according to the time-dependent SIR distribution. If the received SIR exceeds a predefined threshold $\theta$, the packet is transmitted successfully, and removed from the queue. Otherwise, the transmission fails and the packet remains in the queue waiting for retransmission in the next time slot until being successfully received. We assume that there is an instantaneous error-free feedback channel at each link, so that the instantaneous SIR and the result of each transmission, success or failure, are perfectly known at the transmitter side. There is no limit on the number of possible retransmissions. However in practice, the number of needed retransmissions remains low when the system is stable [12]. At each time slot, the BSs with empty buffer remain silent to reduce power consumption and inter-cell interference. Let $\Phi_t$ be the set of BSs that are transmitting in the time slot $t \in \mathbb{N}$. We have $\Phi_t \subseteq \Phi$, and $\Phi_t = \Phi$ when all BSs are active, at time $t$. A snapshot of a realization of an HPPP with queue state at a node is presented in Fig. 1.

### B. Signal-to-interference ratio

An interference limited network is assumed, i.e. neglecting the noise. By the Slivnyak's theorem [14], it is sufficient to focus on the SIR of a typical UE at the origin. With its tagged BS located at $x_0$, the received SIR experienced by the typical UE at time slot $t$ is

$$\gamma_t = \frac{h_{x_0,t} \|x_0\|^{-\alpha}}{\sum\limits_{x \in \Phi \setminus x_0} h_{x,t} \|x\|^{-\alpha} \mathbb{1}(x \in \Phi_t)} \tag{1}$$

where $h_{x_0,t} \sim \exp(1)$ is the exponential channel gain between the typical UE and its tagged BS, $\|x\|$ is the distance from the interfering BS at $x$ to the origin, $h_{x,t}$ is the exponential channel gain between the typical UE and the interfering BS at position $x$ and time slot $t$, with mean 1, and $\alpha$ is the path loss exponent.

Moreover, we note $q_t$ the probability

$$q_t = \mathbb{P}_{\mathbb{1}(x \in \Phi_t)}(\mathbb{1}(x \in \Phi_t) = 1) \tag{2}$$

which can be seen as the fraction of active interfering BS at time slot $t$, or equivalently the probability that a randomly chosen BS is active at time slot $t$.

## III. $\epsilon$-STABLE REGION

The $\epsilon$-stable region gives the maximum arrival rate beyond which the probability for the queue at typical UE to be unstable exceeds a threshold $\epsilon$. A queue becomes unstable if the arrival rate exceeds the average long-term departure rate. To illustrate this issue, we first define the transmit success probability as follows.

**Definition 1.** *Given a SIR threshold $\theta$ and a given realization of the PPP, the transmit success probability at the typical BS $x_0$ at time slot $t$ is*

$$\mu_t = \mathbb{P}\left( \frac{h_{x_0} \left\| x_0 \right\|^{-\alpha}}{\sum\limits_{x \in \Phi \setminus x_0} h_x \left\| x \right\|^{-\alpha} \mathbb{1}(x \in \Phi_t)} \geq \theta \middle| \Phi \right) \tag{3}$$

**Lemma 1.** *The transmit success probability experienced by the typical UE at time $t$ is*

$$\mu_t = \prod_{x \in \Phi \setminus x_0} \left( \frac{q_t}{1 + \theta \left\| x_0 \right\|^{\alpha} \left\| x \right\|^{-\alpha}} + 1 - q_t \right) \tag{4}$$

*Proof.* See Appendix A. □

Lemma 1 quantifies how the transmit success probability behaves at a given time slot and depends on the traffic. The queue states are affecting the transmit success probability via the probability $q_t$. As $q_t$ decreases, less interferers are active in the network, and hence, the aggregate interference decreases and $\mu_t$ increases at typical BS.

**Definition 2** ( [10, Definition 1])**.** *Let $\xi$ be the arrival rate. For any $\epsilon \in [0,1]$, the $\epsilon$-stability region $\mathcal{S}_\epsilon$ is defined as*

$$\mathcal{S}_\epsilon = \left\{ \xi \in [0,1] : \mathbb{P}\left\{ \lim_{T \to \infty} \frac{1}{T} \sum_{t=1}^{T} \mu_t \leq \xi \right\} \leq \epsilon \right\} \tag{5}$$

We define $\xi_c$ as $\xi_c = \sup \mathcal{S}_\epsilon$. The network is $\epsilon$-stable if and only if $\xi \leq \xi_c$.

*1) Lower and upper bounds:* Deriving the $\epsilon$-stability region $\mathcal{S}_\epsilon$ boils down to obtain the critical arrival rate $\xi_c$. It is non-trivial to obtain the closed-form of (5) since the transmit success probability is time dependent. Instead, the upper and lower bound for $\epsilon$-stable region are given by the following lemma.

**Lemma 2.** *Considering the dynamic downlink cellular network introduced above, the critical arrival rate $\xi_c$ can be bounded as follows*

$$\xi_c^l \leq \xi_c \leq \xi_c^u \tag{6}$$

*where*

$$\xi_c^z = \sup\left\{ \xi \in [0,1] : \frac{1}{2} - \frac{1}{\pi} \times \int_0^\infty \frac{1}{w} \mathrm{Im}\left\{ \frac{\xi^{-iw}}{g_z(\theta)} \right\} dw \leq \epsilon \right\}$$

*with $z \in \{l, u\}$ and $g_l(\theta) = {}_2F_1(iw, -\frac{2}{\alpha}; 1 - \frac{2}{\alpha}; -\theta)$ for $\xi_c^l$, and $g_u(\theta) = 1 + \int_1^\infty \left[ 1 - \left( 1 - \frac{\xi\theta}{\theta + v^{\alpha/2}} \right)^{iw} \right] dv$ for $\xi_c^u$.*

*Proof.* See Appendix B. □

The upper bound $\xi_c^u$ is obtained by defining a favorable system where if the transmission of a packet fails, this packet is dropped instead of being re-transmitted. The transmitters only serve newly arrived packets at each time slot, if any, and then are active with probability $q_t = \xi$. In the favorable case, the dropped packet does not lead to an unstable network. This condition is not acceptable in practice, but is introduced here only to derive the upper bound.

The lower bound $\xi_c^l$ is obtained when all BSs keep transmitting all the time, i.e., $q_t = 1,\ \forall t \in \mathbb{N}$, which leads to the highest interference and the lowest transmit success probability in (3).

*2) Approximation of $\xi_c$:* A modified definition of the $\epsilon$-stable region, instead of (5), is given by

$$\mathcal{S}_\epsilon = \left\{ \xi \in [0,1] : \mathbb{P}\left\{ \lim_{t \to \infty} \mu_t \leq \xi \right\} \leq \epsilon \right\} \tag{7}$$

Under this definition, we ignore the initial period of transient values of $\mu_t$, and only characterize the $\epsilon$-stable region when time goes to infinity. The new region is simpler to handle compared with (5). Before delving into the solution details, we make the following assumption.

**Assumption 1.** *The BSs are assumed to be activated independently with probability $q = \lim\limits_{t \to \infty} q_t$ when time goes to infinity, and thus the stable transmit success probability is $\mu = \lim\limits_{t \to \infty} \mu_t$.*

This assumption is reasonable because the effect of small scale fading is independent with time and the positions of UEs and BSs remain constant during the time evolution.

From the temporal perspective, a generic transmission link can be abstracted to a queue with service rate given by $\mu_t$ and arrival rate given by $\xi$. The traffic evolution at typical BS $x_0$ can be modeled as a DTMC in Fig. 2 with $\bar{\xi} = 1 - \xi$ and $\bar{\mu}_t = 1 - \mu_t$. The state space is made of the number of packets in the queue and takes value in $\{0, 1, 2, \cdots\}$. State 0 represents the empty buffer event. When the buffer is in this state, the transmitter remains silent. When the queues evolve up to the convergence, i.e., the DTMC reaches the stationary distribution, the number of active transmitters stabilizes and does not evolve with time. Note that $q$ is the complementary probability for the queue to be in state 0 when DTMC is stationary.

**Lemma 3.** *[9] Under fixed arrival and departure rates, $\xi$ and $\mu$ respectively, the active probability at a randomly chosen BS conditioned on $\Phi$ is*

$$q = \begin{cases} \xi/\mu, & \text{if } \mu > \xi, \\ 1, & \text{if } \mu \leq \xi. \end{cases} \tag{8}$$

According to the relative values of $\mu$ and $\xi$, a randomly chosen BS has a probability of $\xi/\mu$ to be active if its arrival rate is less than the departure rate, and is always active in the opposite case. It is important to note when $\mu < \xi$ then $q = 1$ and all the queue lengths and average queue delays grow up to infinity, corresponding to an unstable network.

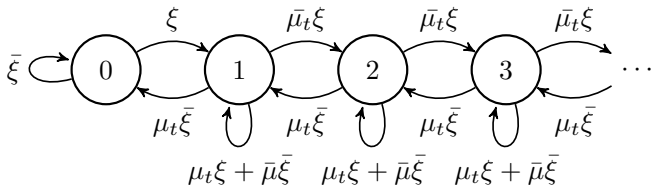


Figure 2. DTMC model.

Thanks to Assumption 1 and Lemma 3, we are ready to present the approximation of the $\epsilon$-stable region in downlink cellular networks.

**Theorem 1.** *Considering the dynamic downlink cellular network introduced above and definition in* (7)*, the approximated critical arrival rate of $\epsilon$-stable region can be characterized as follows*

$$\tilde{\xi}_c = \sup\left\{\xi \in [0,1] : \frac{1}{2} - \frac{1}{\pi} \times \int_0^\infty \frac{1}{w} \mathrm{Im}\left\{\frac{\xi^{-iw}}{1+\int_1^\infty \left[1-\left(1-\frac{\mathbb{E}[q]\theta}{\theta+v^{\alpha/2}}\right)^{iw}\right] dv}\right\} dw \leq \epsilon\right\} \tag{9}$$

*where $\mathbb{E}[q] = \frac{\xi}{1-\theta\xi\rho(\theta,\alpha)}$ if $\frac{1}{1+\theta\rho(\theta,\alpha)} > \xi$, and $\mathbb{E}[q] = 1$ otherwise, and $\rho(\alpha,\theta) = \int_1^\infty [\theta + u^{\frac{\alpha}{2}}]^{-1} du$.*

*Proof.* See appendix C. □

The expression in (9) quantifies how the key features of a dynamic network, i.e., interference, SIR receiving threshold and traffic profile, affect the distribution of the $\epsilon$-stable region. Several remarks regarding Theorem 1 are in order.

**Remark 1.** *The upper and lower bound of the critical arrival rate in Lemma 2 corresponds to $\mathbb{E}[q] = \xi$ and $\mathbb{E}[q] = 1$ in Theorem 1, respectively.*

**Remark 2.** *When the SIR receiving threshold $\theta \to 0$, for all $\epsilon \geq 0$, the critical arrival rate approaches to 1. Letting $\theta \to 0$ Theorem 1 becomes*

$$\begin{aligned}\lim_{\theta\to 0} \tilde{\xi}_c &= \sup\left\{\xi \in [0,1] : \frac{1}{2} - \frac{1}{\pi}\int_0^\infty \frac{1}{w}\mathrm{Im}\left\{\xi^{-iw}\right\} dw \leq \epsilon\right\} \\ &= \sup\left\{\xi \in [0,1] : \frac{1}{2} + \frac{1}{\pi} \times \frac{\pi}{2}\mathrm{sgn}(\ln \xi) \leq \epsilon\right\} \\ &= 1 \end{aligned} \tag{10}$$

*since $\mathrm{sgn}(\ln \xi) = -1, \forall\ \xi \in (0,1)$. Similar conclusion can be drawn for the upper bound $\xi_c^u$ and lower bound $\xi_c^l$. According to the squeeze theorem [15], Remark 2 is obtained.*

Remark 2 illustrates that a transmission attempt is almost surely successful when $\theta \to 0$, thus the admissible critical arrival rate approaches 1.

## IV. Numerical Results

In this section, we validate the accuracy of our analysis through simulations, and explore the impact of traffic condition on network performance from several aspects. Unless otherwise mentioned, the following parameters are used throughout this section: path loss exponent $\alpha = 4$, BS density $\lambda = 0.25$, and packet arrival rate $\xi \in [0,1]$ packet/slot.

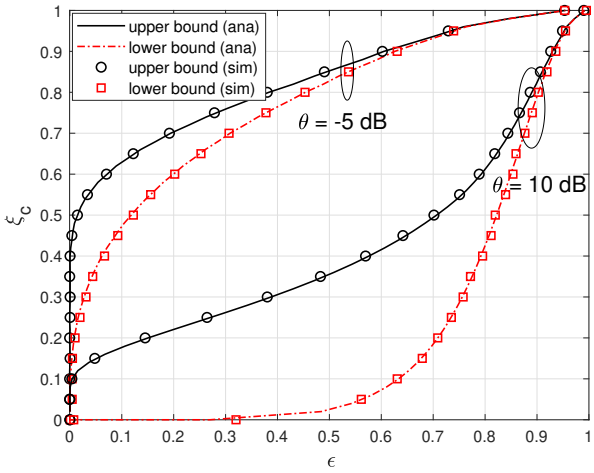


Figure 3. Upper and lower bounds of the $\epsilon$-stable region.

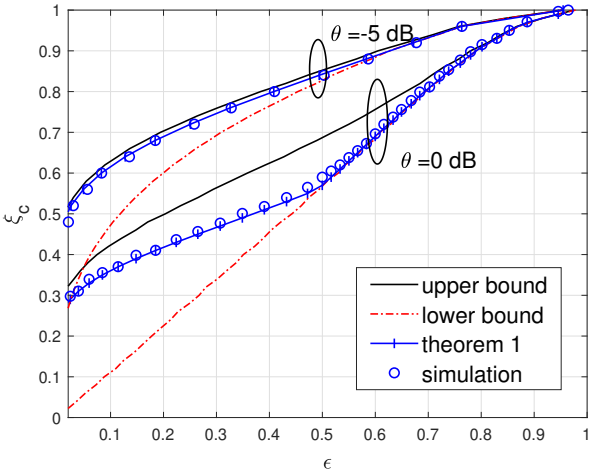


Figure 4. The approximation and bounds of the $\epsilon$-stable region.

Three simulation scenarios are considered. (i) The original system described in section II. For each network realization, the queues are let to evolve up to the convergence, i.e., when the number of active transmitters stabilizes and does not evolve with time. Then a new network realization is drawn and the process repeats; (ii) The full load case, where all BSs keep transmitting all the time, leading to the lower bound described in Lemma 2; (iii) The favorable system, where a randomly chosen BS is active with probability $\xi$, leading to the upper bound described in Lemma 2.

Fig. 3 plots the upper and lower bounds of the $\epsilon$-stable region w.r.t. $\epsilon$ and labeled on the SIR threshold $\theta$, i.e., $\theta = -5$ dB and $\theta = 10$ dB. The figure shows a perfect match between simulations and the analytical expressions obtained in Lemma 2.

The real critical arrival rate, i.e., the average rate at which the probability to be unstable for a queue exceeds $\epsilon$, lies between these bounds. Next, we observe that the region between upper and lower bounds reduces when $\epsilon$ increases, i.e., the bounds converge to 1 when $\epsilon = 1$ as mentioned in Remark 2. Moreover, the critical arrival rate $\xi_c$ decreases when $\theta$ increases. Indeed, as $\theta$ increases, a transmission has a higher chance to fail when scheduled. Hence, the possible arrival rates, i.e., those for which the network is $\epsilon$-stable, decrease. The figure also reveals that the upper and lower bounds are not tight when $\theta$ is high and $\epsilon$ is low.

Fig. 4 focuses on the approximation of the critical arrival rate $\tilde{\xi}_c$ derived in Theorem 1. The critical arrival rate obtained by simulation is based on Definition 2 and it is compared to the expression in Theorem 1 which is based on (7). We can observe that the critical rate lies between our upper and lower bounds and Theorem 1 reveals to be a good approximation of the true critical rate, as confirmed by the simulations. This observation implies that the transient phase present in Definition 5 but not in (7), has a negligible effect on the critical arrival rate. Moreover, it is observed that the critical arrival rate $\tilde{\xi}_c$ is close to the upper bound $\xi_c^u$ when $\theta$ is relatively small, i.e., $\theta = -5$ dB. This is because decreasing $\theta$ increases the opportunity of a successful transmission. Thus the active probability of the typical BS in the real case is much closer to the active probability in the favorable system. Last but not least, the numerical computation of (9) is far faster than running Monte-Carlo simulations, i.e., few minutes compared to several days of simulations.

## V. CONCLUSION

In this work, we have proposed a full characterization of the $\epsilon$-stable region in a dynamic downlink cellular network. We have bounded the critical arrival rate, i.e., the rate at which the queue becomes unstable, and also presented an approximation of this rate. These results allow a quick assessment of the proportion of queues that are in outage on average when the network deployment is modeled with PPP and the network traffic is modeled with DTMC.

In a real-world environment, the network dynamically adjusts its radio parameters, such as BS transmit power or modulation and coding schemes, depending on the traffic conditions. However, the characterization of $\epsilon$-stable regions under complex settings is quite challenging and requires the introduction of Markov decision processes and reinforcement learning strategies in the analysis. This opens new doors in research associating stochastic geometry and machine learning and is left for further works.

## APPENDIX

### A. Proof of Lemma 1

Given the typical UE received data at time slot $t$, its transmit success probability is written as

$$\mu_t = \mathbb{P}^{x_0}\left(\frac{h_{x_0,t}\left\|x_0\right\|^{-\alpha}}{\sum\limits_{x\in\Phi\setminus x_0} h_{x,t}\left\|x\right\|^{-\alpha}\mathbb{1}(x\in\Phi_t)} > \theta \middle| \Phi\right)$$

$$= \mathbb{E}_{\{h_x\},\mathbb{1}(x\in\Phi_t)}\left[\exp\left(-s\sum_{x\in\Phi\setminus x_0} h_x\left\|x\right\|^{-\alpha}\mathbb{1}(x\in\Phi_t)\right)\middle|\Phi\right]$$

$$\overset{a}{=} \mathbb{E}_{\{h_x\},\mathbb{1}(x\in\Phi_t)}\left[\prod_{x\in\Phi\setminus x_0}\exp\Big(-sh_x\left\|x\right\|^{-\alpha}\mathbb{1}(x\in\Phi_t)\Big)\middle|\Phi\right]$$

$$= \mathbb{E}_{\mathbb{1}(x\in\Phi_t)}\left[\prod_{x\in\Phi\setminus x_0}\frac{1}{1+s\left\|x\right\|^{-\alpha}\mathbb{1}(x\in\Phi_t)}\middle|\Phi\right]$$

$$\overset{b}{=} \prod_{x\in\Phi\setminus x_0}\left(\frac{q_t}{1+\theta\left\|x_0\right\|^{\alpha}\left\|x\right\|^{-\alpha}}+1-q_t\right) \tag{11}$$

where (a) follows from the i.i.d. hypothesis of $h_x$ and further independence from the point process $\Phi$, and (b) follows from the definition $q_t = \mathbb{P}(\mathbb{1}(x\in\Phi_t)=1)$.

### B. Proof of Lemma 2

*a) Lower bound $\xi_c^l$:* Let $\mu^l$ be the transmit success probability experienced by the typical UE in the full load case, it follows

$$\mu^l = \mathbb{E}_{\{h_{x_0}\},\{h_x\}}\left[\mathbb{P}\left(\frac{h_{x_0}\left\|x_0\right\|^{-\alpha}}{\sum\limits_{x\in\Phi\setminus x_0} h_x\left\|x\right\|^{-\alpha}}\geq\theta\middle|\Phi\right)\right]$$

$$= \prod_{x\in\Phi\setminus x_0}\left(\frac{1}{1+\theta\left\|x_0\right\|^{\alpha}\left\|x\right\|^{-\alpha}}\right) \tag{12}$$

Define $Y^l \triangleq \ln(\mu^l)$, then the moment generating function of $Y^l$ is

$$\varphi_{Y^l}(s) = \mathbb{E}_{\Phi}\left[\prod_{x\in\Phi\setminus x_0}\left(\frac{1}{1+\theta\left\|x_0\right\|^{\alpha}\left\|x\right\|^{-\alpha}}\right)^s\right]$$

$$\overset{a}{=} \mathbb{E}_{\Phi}\left[\exp\left(-\lambda\int_{\|x_0\|}^{\infty}\left[1-\left(\frac{1}{1+\theta\left\|x_0\right\|^{\alpha}\|x\|^{-\alpha}}\right)^s\right]d\|x\|\right)\right]$$

$$\overset{b}{=} \left[1+\int_1^{\infty}\left[1-\left(\frac{1}{1+\theta v^{-\frac{\alpha}{2}}}\right)^s\right]dv\right]^{-1}$$

$$\overset{c}{=} \left[-\frac{2}{\alpha}\int_0^1\left[1-\left(\frac{1}{1+\theta t}\right)^s\right]t^{-\frac{2}{\alpha}-1}dt\right]^{-1}$$

$$\overset{d}{=} \left({}_2F_1(s,-\frac{2}{\alpha};1-\frac{2}{\alpha};-\theta)\right)^{-1} \tag{13}$$

where (a) follows from the probability generation functional of the PPP; (b) is obtained by using the PDF of $\|x_0\|$, which is $f_{||x_0||}(r) = 2\pi\lambda r e^{\pi\lambda r^2}dr$ and the change of variable $v^{\frac{1}{2}} = \frac{\|x\|}{\|x_0\|}$; (c) is obtained using the change of variable $v^{-\frac{\alpha}{2}} = t$. The integral in (c) can be shown, after some algebraic manipulations, equal to the Gauss hypergeometric function in (d) [16, Section 9.11, pp 1005].

The CDF of $Y^l$, denoted by $\mathbb{P}(Y^l < y)$, follows from the Gil-Pelaez's Theorem as

$$\mathbb{P}(Y^l < \ln(u)) = \frac{1}{2} - \frac{1}{\pi}\int_0^{\infty}\frac{\mathrm{Im}[u^{-iw}\varphi_{Y_l}(iw)]}{w}dw \tag{14}$$

The corresponding lower bound of the $\epsilon$-stability region is

$$\mathcal{S}_\epsilon^l = \Bigg\{\xi \in [0,1]\colon \frac{1}{2} - \frac{1}{\pi}\int_0^\infty \frac{1}{w} \times \operatorname{Im}\left\{\frac{\xi^{-iw}}{{}_2F_1(iw, -\frac{\alpha}{2}; 1-\frac{\alpha}{2}; -\theta)}\right\} dw \le \epsilon\Bigg\} \tag{15}$$

*b) Upper bound $\xi_c^u$:* Let $\mu^u$ be the transmit success probability experienced by the typical UE in the favorable system, it follows

$$\begin{aligned}\mu^u =& \mathbb{E}\left[\exp\left(-\theta \left\|x_0\right\|^\alpha \sum_{x\in\Phi\setminus x_0} h_x \mathbb{1}(x\in\Phi_t) \left\|x\right\|^{-\alpha}\right)\middle|\Phi\right] \\ =& \prod_{x\in\Phi\setminus x_0}\left(\frac{\xi}{1+\theta\left\|x_0\right\|^\alpha \left\|x\right\|^{-\alpha}} + 1 - \xi\right)\end{aligned} \tag{16}$$

We define $Y^u$ as $Y^u \triangleq \ln(\mu^u)$, and follow similar steps as in (13), the moment generating function of $Y_u$ is

$$\varphi_{Y^u}(s) \quad = \left[1 + \int_1^\infty \left[1 - \left(1 - \frac{\xi\theta}{\theta + v^{\frac{\alpha}{2}}}\right)^s\right] dv\right]^{-1} \tag{17}$$

According to the Gil-Pelaez's Theorem, the probability of $\mu^u$ be lower than the average arrival rate $\xi$ is

$$\mathbb{P}\{\mu^u < \xi\} = \frac{1}{2} - \frac{1}{\pi}\int_0^\infty \frac{1}{w}\operatorname{Im}\{\xi^{-iw}\varphi_{Y^u}(iw)\} dw \tag{18}$$

The corresponding upper bound of $\epsilon$-stable region is obtained and leads to the result in Lemma 2.

### C. Proof of Theorem 1

Based on Lemma 1 and assumption 1, the stable transmit success probability has the expression

$$\mu = \prod_{x\in\Phi\setminus x_0}\left(\frac{q}{1+\theta\left\|x_0\right\|^\alpha \left\|x\right\|^{-\alpha}} + 1 - q\right). \tag{19}$$

Defining $Y \triangleq \ln\mu$, the moment generating function of $Y$ is

$$\begin{aligned}&\mathbb{E}\left[\exp(sY)\right] \\ &= \mathbb{E}_\Phi\left[\prod_{x\in\Phi\setminus x_0}\left(\frac{q}{1+\theta\left\|x_0\right\|^\alpha\left\|x\right\|^{-\alpha}} + 1 - q\right)^s\right] \\ &\overset{a}{=} \mathbb{E}_\Phi\left[e^{-\lambda\int_{\|x_0\|}^\infty\left[1-\left(\frac{q}{1+\theta\|x_0\|^\alpha\|x\|^{-\alpha}}+1-q\right)^s\right]d\|x\|}\right] \\ &\overset{b}{=} \int_0^\infty 2\pi\lambda r e^{-\lambda\pi r^2}\exp\left(-\lambda\pi r^2\int_1^\infty\left[1-\left(\frac{q}{1+\theta v^{-\frac{\alpha}{2}}}\right)^s\right]dv\right)dr \\ &= \left[1 + \int_1^\infty\left[1-\left(1-\frac{q\theta}{\theta+v^{\frac{\alpha}{2}}}\right)^s\right]dv\right]^{-1}\end{aligned} \tag{20}$$

where steps (a) and (b) are the same as those in (13).

Aforesaid Lemma 3, $\mathbb{E}_\Phi[q] = \xi/\mathbb{E}_\Phi[\mu], \forall\ \mathbb{E}_\Phi[\mu] > \xi$. And it can be noticed that $\mathbb{E}_\Phi[\mu]$ is the particular case when $s = 1$ in (20). After straightforward algebraic manipulations, we have

$$\mathbb{E}[q] = \begin{cases}\frac{\xi}{1-\theta\xi\rho(\theta,\alpha)}, & \text{if } \frac{1}{1+\theta\rho(\theta,\alpha)} > \xi \\ 1, & \text{if } \frac{1}{1+\theta\rho(\theta,\alpha)} \le \xi\end{cases} \tag{21}$$

where $\rho(\alpha,\theta) = \int_1^\infty [\theta + u^{\frac{\alpha}{2}}]^{-1} du$.

The CDF of $Y$, denoted by $F_Y(u) = \mathbb{P}[Y \le u]$, follows from the Gil-Pelaez's Theorem as

$$\begin{aligned}F_Y(u) &= \mathbb{P}(Y < \ln(u)) \\ &= \frac{1}{2} - \frac{1}{\pi}\int_0^\infty \frac{1}{w}\operatorname{Im}\left\{\frac{u^{-iw}}{1+\int_1^\infty\left[1-\left(1-\frac{k\theta}{\theta+v^{\alpha/2}}\right)^{iw}\right]dv}\right\} dw\end{aligned}$$

and the proof is complete.

## REFERENCES


[1] H. ElSawy and E. Hossain, "On stochastic geometry modeling of cellular uplink transmission with truncated channel inversion power control," *IEEE Transactions on Wireless Communications*, vol. 13, no. 8, pp. 4454–4469, Aug 2014.

[2] J. G. Andrews, F. Baccelli, and R. K. Ganti, "A tractable approach to coverage and rate in cellular networks," *IEEE Transactions on Communications*, vol. 59, no. 11, pp. 3122–3134, 2011.

[3] H. S. Dhillon, R. K. Ganti, and J. G. Andrews, "Load-aware modeling and analysis of heterogeneous cellular networks," *IEEE Transactions on Wireless Communications*, vol. 12, no. 4, pp. 1666–1677, 2013.

[4] B. Blaszczyszyn, M. Jovanovic, and M. K. Karray, "Performance laws of large heterogeneous cellular networks," in *International Symposium on Modeling and Optimization in Mobile, Ad Hoc, and Wireless Networks (WiOpt)*, Mumbai, India, 2015, pp. 597–604.

[5] N. Jiang, Y. Deng, X. Kang, and A. Nallanathan, "Random access analysis for massive iot networks under a new spatio-temporal model: A stochastic geometry approach," *IEEE Transactions on Communications*, vol. 66, no. 11, pp. 5788–5803, Nov 2018.

[6] F. Baccelli and P. Brémaud, *Elements of queueing theory: Palm Martingale calculus and stochastic recurrences*, 2nd ed., ser. Applications of Mathematics. Springer, Berlin, Heidelberg, 2003.

[7] A. AlAmmouri, J. G. Andrews, and F. Baccelli, "Stability of wireless random access systems," in *Annual Allerton Conference on Communication, Control, and Computing*, Monticello, IL, USA, Oct. 2019, pp. 1190–1197.

[8] M. Gharbieh, H. Elsawy, A. Bader, and M. S. Alouini, "Spatiotemporal Stochastic Modeling of IoT Enabled Cellular Networks: Scalability and Stability Analysis," *IEEE Transactions on Communications*, vol. 65, no. 8, pp. 3585–3600, 2017.

[9] Q. Liu, J.-Y. Baudais, and P. Mary, "A tractable coverage analysis in dynamic downlink cellular networks," in *International Workshop on Signal Processing Advances in Wireless Communications (SPAWC)*, Atlanta, Georgia, USA, May 2020.

[10] Y. Zhong, M. Haenggi, T. Q. S. Quek, and W. Zhang, "On the stability of static poisson networks under random access," *IEEE Transactions on Communications*, vol. 64, no. 7, pp. 2985–2998, July 2016.

[11] M. Haenggi, "The Meta Distribution of the SIR in Poisson Bipolar and Cellular Networks," *IEEE Transactions on Wireless Communications*, vol. 15, no. 4, pp. 2577–2589, 2016.

[12] Q. Liu, J.-Y. Baudais, and P. Mary, "Queue analysis with finite buffer by stochastic geometry in downlink cellular networks," in *Vehicular Technology Conference (VTC)*, Helsinki, Sweden, Apr. 2021.

[13] H. H. Yang, G. Geraci, Y. Zhong, and T. Q. Quek, "Packet throughput analysis of static and dynamic tdd in small cell networks," *IEEE Wireless Communications Letters*, vol. 6, no. 6, pp. 742–745, 2017.

[14] H. ElSawy, E. Hossain, and M. Haenggi, "Stochastic geometry for modeling, analysis, and design of multi-tier and cognitive cellular wireless networks: A survey," *IEEE Communications Surveys Tutorials*, vol. 15, no. 3, pp. 996–1019, Third 2013.

[15] H.H. Sohrab, *Basic Real Analysis*, 2nd ed. Springer, 2014.

[16] I.S. Gradshteyn and I.M. Ryzhik, *Table of Integrals, Series, and Products*, 7th ed. Elsevier, Academic Press, 2007.